

# Supporting Material for:

## Electrochemical reaction in single layer MoS<sub>2</sub>: nanopores opened atom by atom

J. Feng<sup>1</sup>, K. Liu<sup>1</sup>, M. Graf<sup>1</sup>, M. Lihter<sup>1,2</sup>, R. D. Bulushev<sup>1</sup>, D. Dumcenco<sup>3</sup>, D.T.L. Alexander<sup>4</sup>, D. Krasnozhan<sup>3</sup>, T. Vuletic<sup>2</sup>, A. Kis<sup>3</sup>, and A. Radenovic<sup>1</sup>

<sup>1</sup>Laboratory of Nanoscale Biology, Institute of Bioengineering, School of Engineering, EPFL, 1015 Lausanne, Switzerland

<sup>2</sup>Institut za fiziku, Bijenička 46, Zagreb, Croatia

<sup>3</sup>Laboratory of Nanoscale Electronics and Structure, Institute of Electrical Engineering, School of Engineering, EPFL, 1015 Lausanne, Switzerland

<sup>4</sup>Centre Interdisciplinaire de Microscopie Électronique (CIME), 1015 Lausanne, Switzerland

## Table of contents

1. Experimental methods (setup, CVD MoS<sub>2</sub> growth, transfer of CVD MoS<sub>2</sub> from sapphire to SiNx membrane, graphene CVD growth, finite element analysis model)
2. STEM-EDX analysis of transferred CVD MoS<sub>2</sub> on a supporting SiNx membrane (**SI Fig 1.**)
3. Leakage current of intact MoS<sub>2</sub> membrane below critical voltage (**SI Fig 2.**)
4. Finite element analysis of the electric potential distribution for a 0.3 nm pore in single layer MoS<sub>2</sub> at 800 mV corresponding to the conditions of ECR (**SI Fig 3.**)
5. Current-voltage (IV) characteristic of nanopore created via electrochemical reaction with corresponding (AC) Cs-TEM image. (**SI Fig 4.**)
6. A typical current trace of nanopore formation on graphene membrane using ECR (**SI Fig 5.**)
7. Detailed data analysis of ionic current steps presented in **Fig. 3** together with the (**SI Fig 6.**) showing down-sampled raw ionic current signal with the edge-preserving Chung-Kennedy (CK) filter signal and corresponding pairwise differences distribution (PDD).
8. A reproduced current trace of nanopore formation on MoS<sub>2</sub> membrane using ECR showing discrete steps (**SI Fig 7.**).
9. **Table S1.** The sequence of cleaving MoS<sub>2</sub> unit cells and Mo and S atoms in 21 steps to form the pore
10. Power density spectrum (PSD) noise analysis of ECR fabricated MoS<sub>2</sub> nanopore (**SI Fig 8.**)
11. λ-DNA translocation events through 4 nm ECR fabricated nanopore (**SI Fig 9.**)
12. Simplistic analytical model that relates conductance drops to the number and size of the pore (**SI Fig 10.**)

## Experimental Methods

### Setup

The MoS<sub>2</sub> membranes are prepared using the previously reported procedure<sup>1</sup>. Briefly, 20 nm thick supporting SiN<sub>x</sub> membranes are manufactured using anisotropic KOH etching to obtain 10 μm × 10 μm to 50 μm × 50 μm membranes, with size depending on the size of the backside opening. Focused ion beam (FIB) is used to drill a 50 – 300 nm opening on that membrane. CVD-grown MoS<sub>2</sub> flakes were transferred from sapphire substrates using MoS<sub>2</sub> transfer stage in a manner similar to the widely used graphene transfer method and suspended on FIB opening<sup>2,3</sup>. Membranes are first imaged in the TEM with low magnification in order to check suspended MoS<sub>2</sub> flakes on FIB opening.

For the nanopore fabrication experiments, after mounting in the polymethylmethacrylate (PMMA) chamber, the chips were wetted with H<sub>2</sub>O:ethanol (v:v, 1:1) for at least 20 min. 1 M KCl solution buffered with 10mM Tris-HCl and 1mM EDTA at pH 8.0 was injected in the chamber. A pair of chlorinated Ag/AgCl electrodes was employed to apply the transmembrane voltage and the current between the two electrodes was measured by a FEMTO DLPCA-200 amplifier (FEMTO® Messtechnik GmbH). A low voltage (100 mV) was applied to check the current leakage of the membrane. If the leakage current was below 1 nA, we stepped-up the voltage bias in 100 mV steps (25 s for each step). At a critical voltage we observed the current starting to immediately increase above the leakage level. We use a FPGA card and custom-made LabView software for applying the voltage. The critical voltage was automatically shut-down by a feedback control implemented in LabView program as soon as the desirable conductance was reached. Nanopores were further imaged using a JEOL 2200FS high-resolution transmission electron microscope (HR-TEM). Scanning TEM (STEM) energy dispersive X-ray spectroscopy (EDX) mapping was performed on a ChemiSTEM-equipped FEI Tecnai Osiris transmission electron microscope (TEM). Aberration-corrected TEM micrographs were taken on a FEI Titan Themis 60-300 at 80 keV.

Current–voltage, IV characteristic and DNA translocation were recorded on an Axopatch 200B patch clamp amplifier (Molecular Devices, Inc. Sunnyvale, CA). DNA samples (pNEB193, plasmid 2.7 k bp, New England; λ-DNA, 48 k bp, New England) were diluted by mixing 10 μL of λ-DNA or pNEB stock solution with 490 μL 1 M KCl buffer. We use a NI PXI-4461 card for data digitalization and custom-made LabView software for data acquisition using Axopatch 200B. The sampling rate is 100 kHz and a built-in low-pass filter at 10 kHz is used. Data analysis enabling event detection is

performed offline using a custom open source Matlab code, named OpenNanopore<sup>4</sup> (<http://lben.epfl.ch/page-79460-en.html>).

### **CVD MoS<sub>2</sub> growth**

Monolayer MoS<sub>2</sub> has been grown by chemical vapor deposition (CVD) on c-plane sapphire. After consecutive cleaning by acetone/isopropanol/DI-water the substrates were annealed for 1h at 1000 °C in air. After that, they were placed face-down above a crucible containing ~5 mg MoO<sub>3</sub> (≥ 99.998% Alfa Aesar) and loaded into a furnace with a 32 mm outer diameter quartz tube. CVD growth was performed at atmospheric pressure using ultrahigh-purity argon as the carrier gas. A second crucible containing 350 mg of sulfur (≥ 99.99% purity, Sigma Aldrich) was located upstream from the growth substrates. More details are available in <sup>3</sup>.

### **CVD MoS<sub>2</sub> transfer from sapphire to SiN<sub>x</sub> membrane**

Monolayer MoS<sub>2</sub> grown on sapphire substrate (12 mm by 12 mm) is coated by A8 PMMA (495) and baked at 180 °C. We use a diamond scribe to cut it into 4 pieces. Each piece is immersed into 30%w KOH at 85-90°C for the detachment. It is advisory to use capillary force in the interface between polymer and sapphire to facilitate the detachment and reduce the etching time in the KOH. The detached polymer film was repeatedly in DI water. Lastly, the “fishing” method of graphene transfer can be used to transfer CVD MoS<sub>2</sub> to the target SiN<sub>x</sub> membrane.

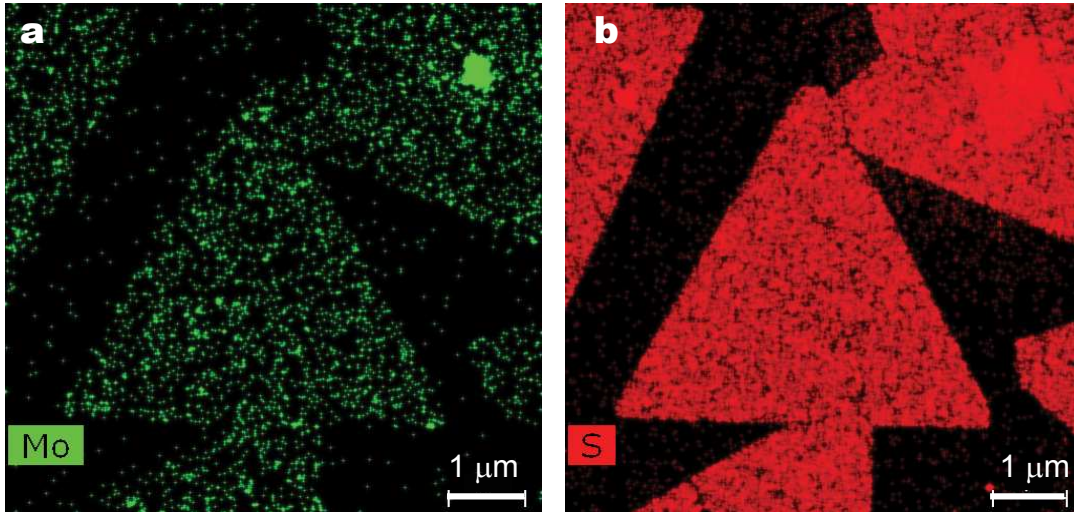
### **CVD graphene growth**

Large-area graphene films are grown on copper foils. The growth takes place under the flow of a methane / argon / hydrogen reaction gas mixture at a temperature of 1000 °C. At the end of the growth, the temperature is rapidly decreased and the gas flow turned off. The copper foils are then coated by PMMA and the copper etched away, resulting in a cm-scale graphene film ready to be transferred on the chips with membranes.

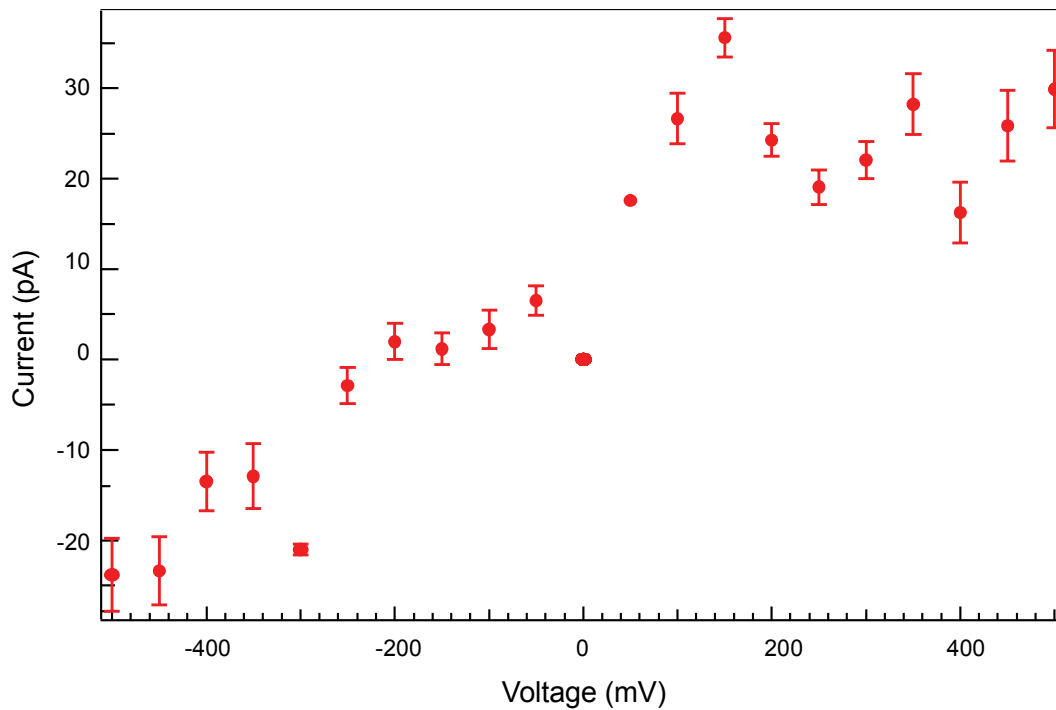
### **Finite element analysis model**

To estimate the potential drop in a defect in a MoS<sub>2</sub> membrane a finite element analysis was performed using COMSOL Multiphysics 4.4b. A coupled set of the Poisson-Nernst-Planck equations was solved in a 3D geometry with axial symmetry. In the modeled configuration cis and trans chambers were connected by a 0.3 nm pore in a 0.7 nm thick membrane suspended on a 50 nm wide and 20 nm thick hole. A 0.3 nm

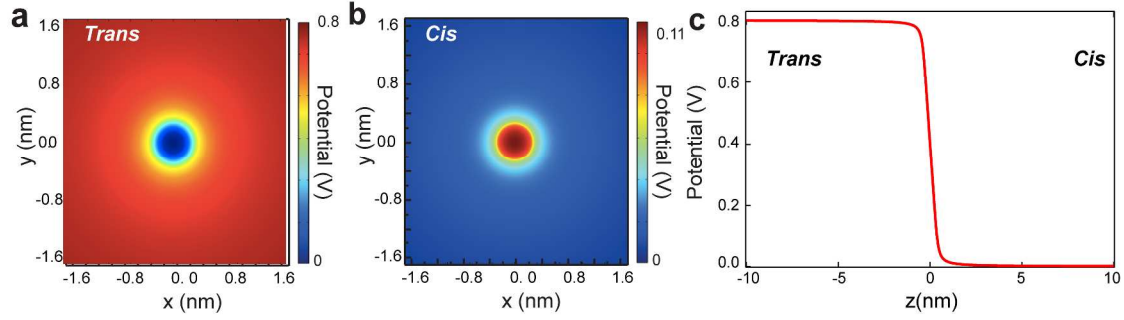
diameter defect can correspond to the absence of a unit cell of MoS<sub>2</sub>. In the model, the applied potential was set to 800 mV and salt concentration was 1 M KCl. The minimal mesh size used was less than 0.2 Å.



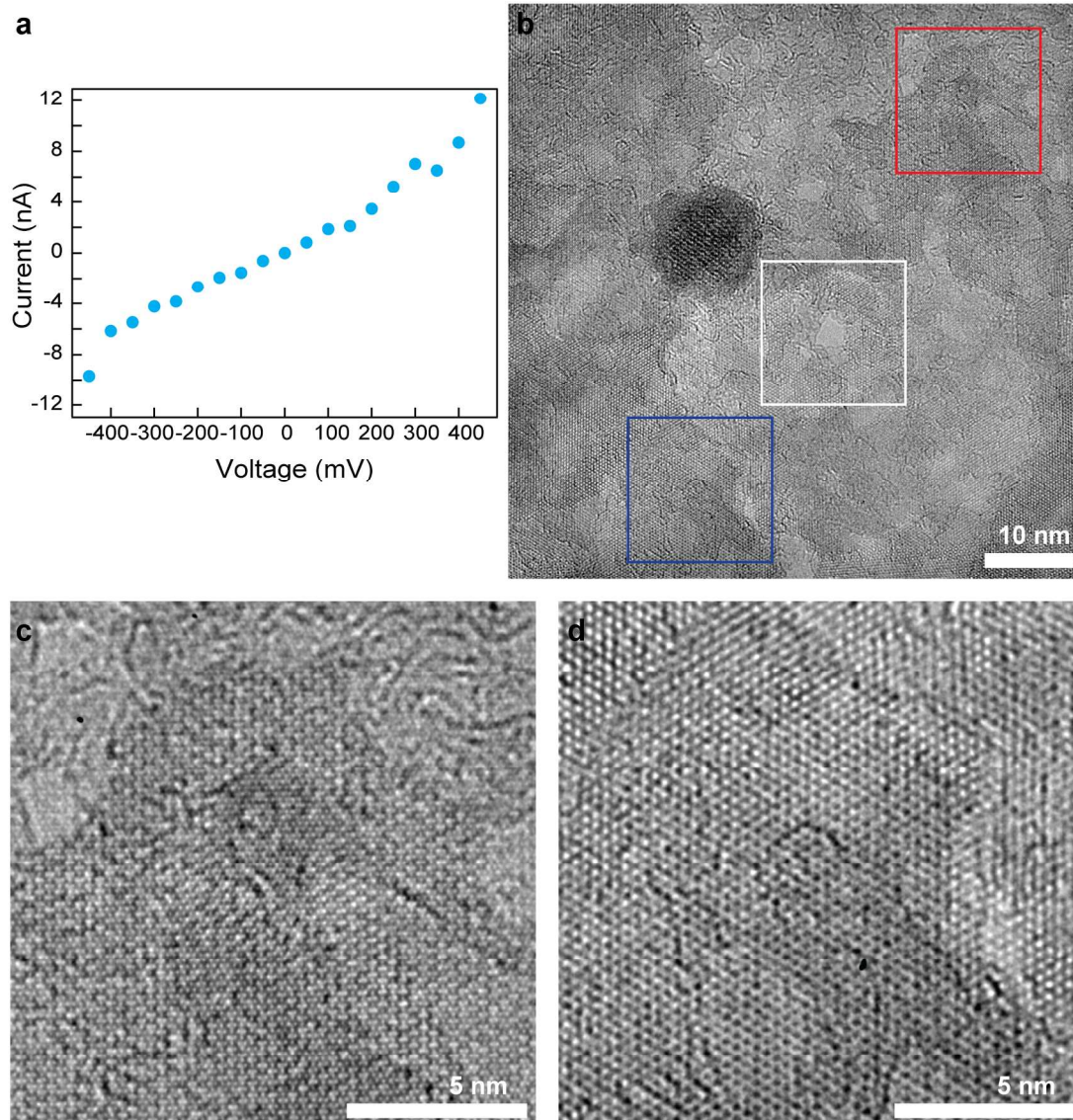
**SI Fig.1** EDX mapping of Mo and S elements in the monolayer MoS<sub>2</sub> film composed of triangular single-crystal domains transferred on the supporting SiN<sub>x</sub> membrane. FEI Tecnai Osiris TEM is operated in the STEM mode at 200 kV to achieve high speed and high sensitivity EDX measurements. To unambiguously decouple S from Mo Electron Energy Loss Spectroscopy (EELS) analysis of the samples would be required.



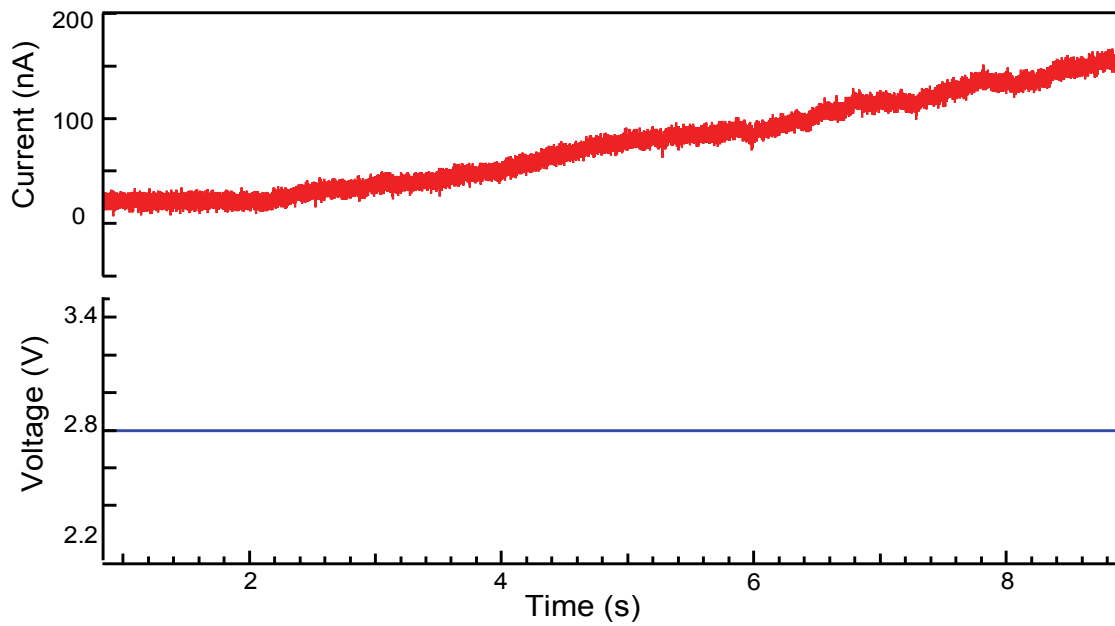
**SI Fig.2** Leakage current-voltage (IV) characteristic of an intact MoS<sub>2</sub> membrane, for voltages below the critical voltage of 800 mV required for ECR. The leakage current depends on the number of the membrane defects. More defects leads to higher current.



**SI Fig.3.** Simulations of the electric potential distribution for the nanopore in two dimensions for a just formed pore having a diameter of 0.3 nm. (a) Electric potential distribution in the *trans* chamber in the immediate vicinity of the membrane surface and (b) in the *cis* chamber. (c) Electric potential distribution as a function of the distance from the pore. The applied potential was set to 800 mV and salt concentration was 1 M KCl.



**SI Fig.4. (a)** Current-voltage (IV) characteristic of nanopore created via electrochemical reaction having conductance of  $\sim 22.8$  nS in 1M KCl which corresponds to nanopore having  $\sim 3.0$  nm diameter. **(b)** Large field of view area (60 nm x 60 nm) Cs-TEM image around the ECR-created nanopore in the middle of the white square, which corresponds to the zoomed region shown in **Fig.2.c**. **(c)** and **(d)** show random (15nm x15 nm ) zooms in the regions indicated by red **(c)** and blue **(d)** squares in **(b)**.



**SI Fig.5** A typical current trace of nanopore formation on graphene membrane using ECR. A much higher transmembrane voltage, 2.8 V has to be applied to graphene to create a nanopore in graphene.



## 6. Detailed data analysis of ionic current steps presented in Fig. 3.

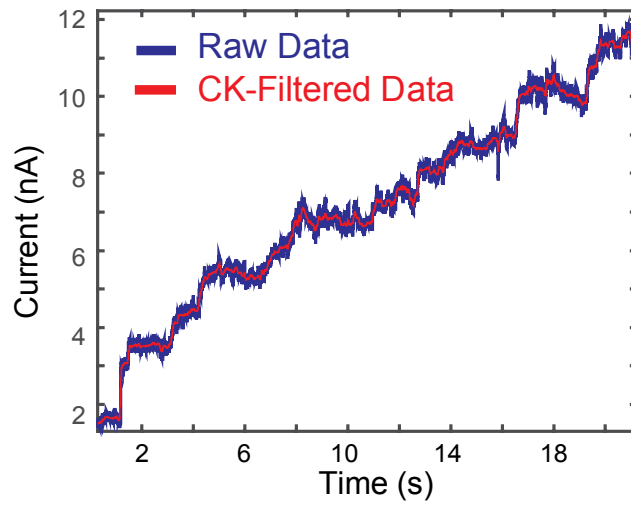
All analysis were implemented in Matlab R2014b. The raw signal was down-sampled to 5 kHz and then filtered using the edge-preserving Chung-Kennedy (CK) filter<sup>5</sup> (Fig. S5a). The pore formation in 21 steps, presented in the journal article on Fig. 3 can be understood in the following way. The growth of the nanopore is due to sequential cleaving of unit cells from MoS<sub>2</sub> lattice. The final pore area is 2.9 nm<sup>2</sup>, which corresponds to 34 unit cells. Increments in the effective pore size  $\Delta A$  are normalized by unit cell size  $u = 0.0864 \text{ nm}^2$ . We round the obtained number  $\Delta N = \Delta A/u$  to the nearest integer, integer +1/3 or integer +2/3 to get  $\Delta X$ , the number of MoS<sub>2</sub> unit cells cleaved during the pore formation process. We assume that 1/3 corresponds to a S<sub>2</sub> group and 2/3 to a Mo atom, corresponding to the partial cleaving of a unit cell. It should be noted that the two S atoms in MoS<sub>2</sub> are stacked vertically and their combined surface area is smaller than that for Mo (which has about 50% larger radius).

The sequence of cleaving MoS<sub>2</sub> unit cells and Mo and S atoms in 21 steps to form the pore is given in the **Table S1**. In order to depict the sequence of the pore formation, the coloring of the lines in the **Table S1** and polygons in the animation based on HRTEM image starts from violet, blue, cyan and green to yellow, orange, brown, red and magenta – akin to the visible spectrum sequence (see *Supporting Movie 1.avi*). Lifetime of the steps in the sequence is given in the **Table 1**. These times are used as the cues for the animation - the pore formation process that we have recorded is thus shown in real-time. Notably, initially irregular pore gradually becomes more symmetrical. White dashed line is a visual aid to denote the progress of pore growth. The atom groups have been selected in the manner to minimize the number of dangling bonds at the edge of the pore. The pore formation sequence is not unique, however, the dangling bond constraint significantly reduces the number of pore formation scenarios and induces more symmetrical pore shape.

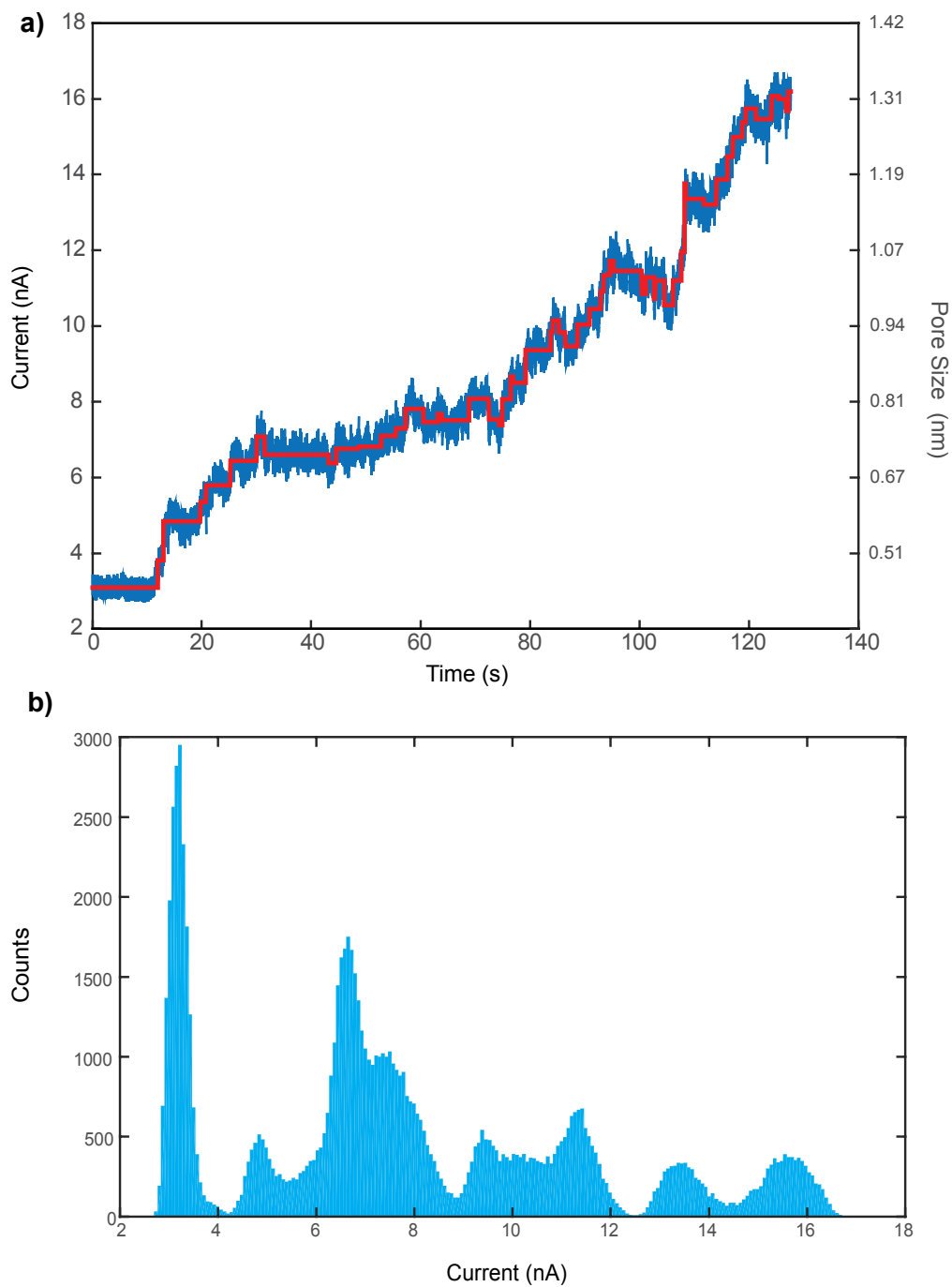


I step [nA]	lifetime [s]	D [nm]	A [nm <sup>2</sup> ]	N	$\Delta A$ [nm <sup>2</sup> ]	$\Delta N$	$\Delta X$ :	atoms/groups cleaved		
0,926	0,1	0,36	0,10	1,16	0,100	1,16	1		MoS <sub>2</sub>	
0,5556	0,2	0,47	0,18	2,04	0,076	0,88	1		MoS <sub>2</sub>	
0,4939	1,7	0,57	0,25	2,92	0,076	0,88	1		MoS <sub>2</sub>	
0,8025	1,0	0,71	0,39	4,53	0,139	1,60	1 2/3		MoS <sub>2</sub>	Mo
0,4939	0,1	0,79	0,49	5,62	0,094	1,09	1		MoS <sub>2</sub>	
0,5556	2,7	0,87	0,60	6,93	0,114	1,31	1 1/3		MoS <sub>2</sub>	S <sub>2</sub>
0,5556	0,8	0,96	0,72	8,34	0,122	1,41	1 1/3		MoS <sub>2</sub>	S <sub>2</sub>
0,8025	3,2	1,08	0,91	10,53	0,189	2,19	2	MoS <sub>2</sub>	MoS <sub>2</sub>	
0,4322	1,5	1,14	1,02	11,79	0,109	1,26	1 1/3		MoS <sub>2</sub>	S <sub>2</sub>
0,3087	0,1	1,18	1,10	12,72	0,080	0,93	1		MoS <sub>2</sub>	
0,3087	0,1	1,23	1,18	13,67	0,083	0,96	1		MoS <sub>2</sub>	
0,3087	1,1	1,27	1,27	14,66	0,085	0,98	1		MoS <sub>2</sub>	
0,6791	1,8	1,36	1,46	16,92	0,195	2,26	2 1/3	MoS <sub>2</sub>	MoS <sub>2</sub>	S <sub>2</sub>
0,4939	0,7	1,43	1,61	18,64	0,149	1,72	1 2/3		MoS <sub>2</sub>	Mo
0,7408	2,7	1,53	1,84	21,35	0,234	2,71	2 2/3	MoS <sub>2</sub>	MoS <sub>2</sub>	Mo
0,6791	0,4	1,62	2,07	23,96	0,226	2,62	2 2/3	MoS <sub>2</sub>	MoS <sub>2</sub>	Mo
0,6173	1,4	1,71	2,29	26,45	0,215	2,49	2 2/3	MoS <sub>2</sub>	MoS <sub>2</sub>	Mo
0,7408	0,1	1,80	2,55	29,57	0,270	3,12	3	MoS <sub>2</sub>	MoS <sub>2</sub>	MoS <sub>2</sub>
0,3087	0,1	1,84	2,67	30,91	0,116	1,34	1 1/3		MoS <sub>2</sub>	S <sub>2</sub>
0,4321	0,1	1,90	2,84	32,84	0,166	1,92	2	MoS <sub>2</sub>	MoS <sub>2</sub>	
0,2469	0,5	1,93	2,93	33,96	0,097	1,12	1		MoS <sub>2</sub>	
Pore:		Diameter:	size nm <sup>2</sup>	cells						
		1,9 nm	2,9	34,0			34			

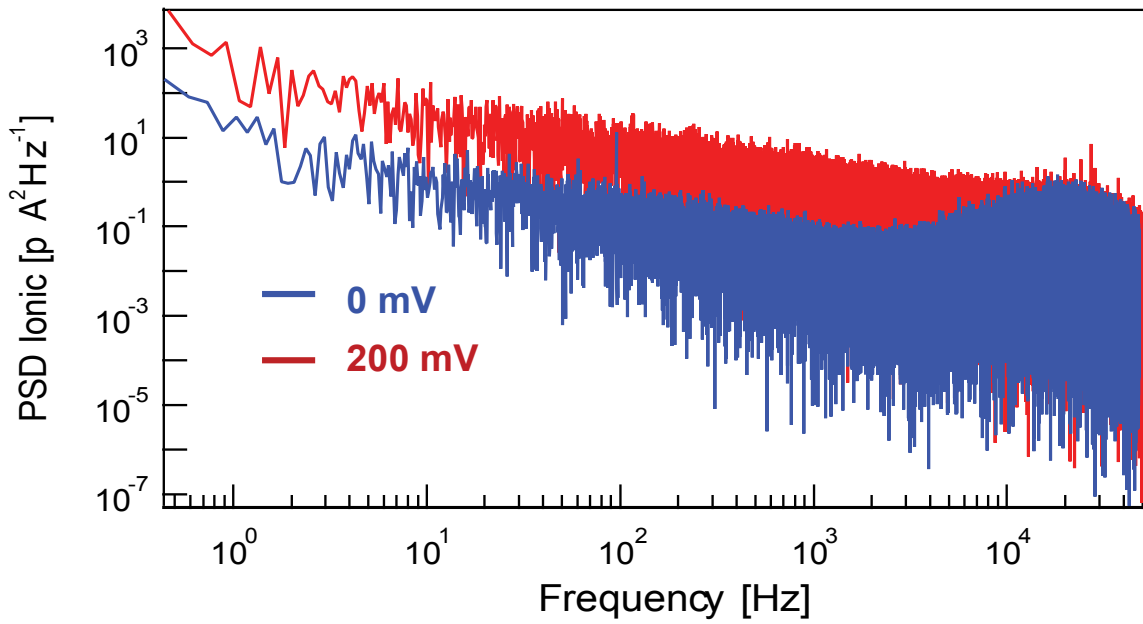
**Table 1.** The sequence of cleaving MoS<sub>2</sub> unit cells and Mo and S atoms in 21 steps to form the pore.



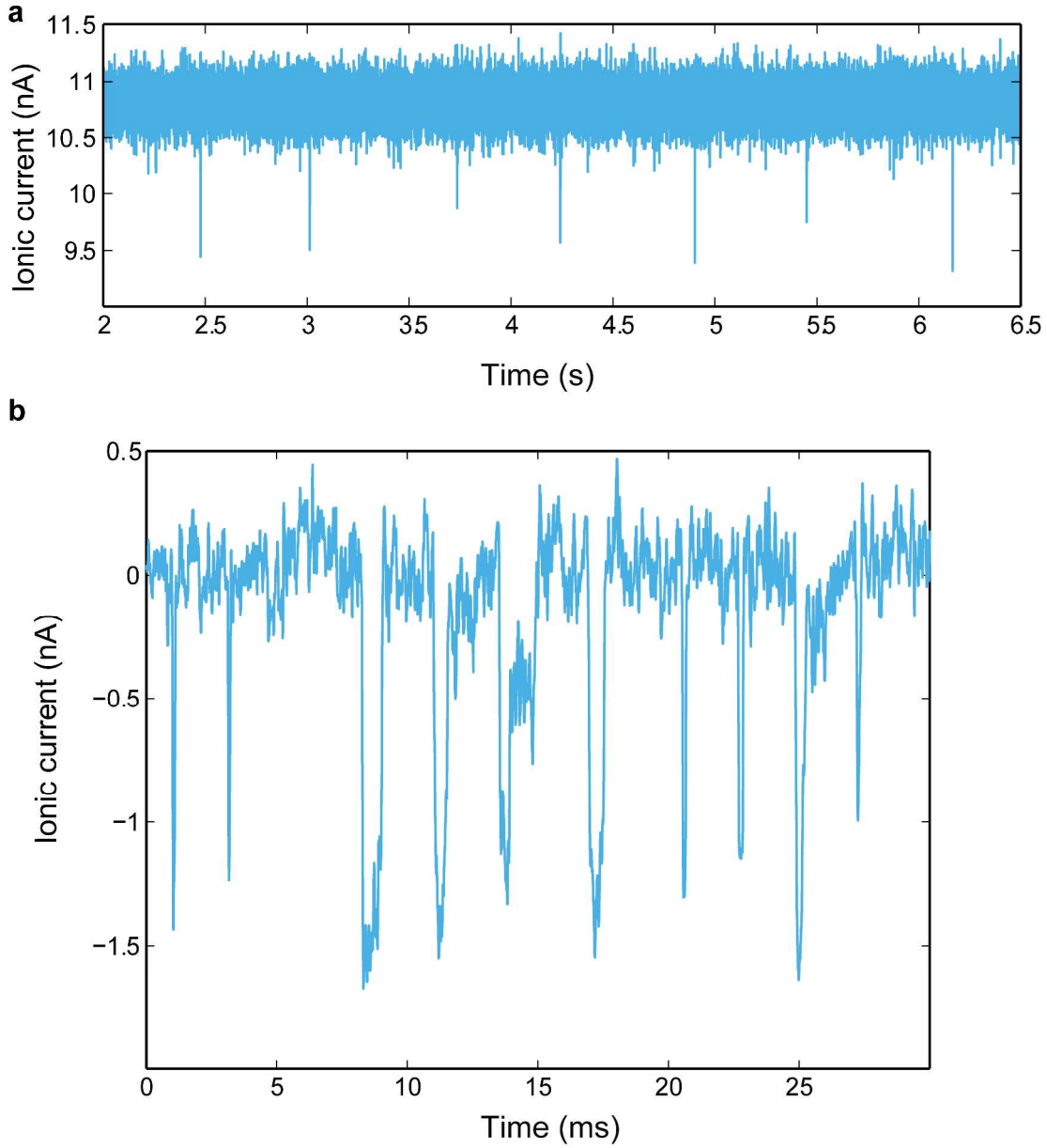
**SI Fig.6** Ionic current signal, obtained during ECR reaction and pore formation. The raw signal was down-sampled to 5 kHz and filtered with the edge-preserving Chung-Kennedy (CK) filter.



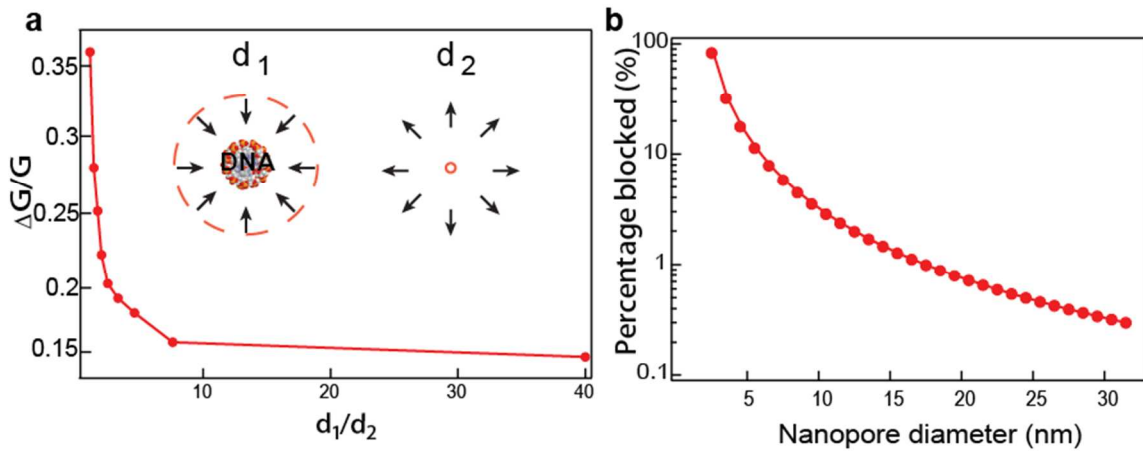
**SI Fig.7 (a)** A reproduced current trace of nanopore formation on MoS<sub>2</sub> membrane using ECR method showing discrete steps at critical potential of 2 V **(b)** Corresponding histogram.



**SI Fig.8** Power density spectrum (PSD) noise analysis of an ECR fabricated  $\text{MoS}_2$  nanopore at the transmembrane voltages of 0 mV (blue) and 200 mV (red), respectively. A short fragment at each voltage of blank ionic current trace is chosen for such an analysis.



**SI Fig.9.** (a) Long trace showing the  $\lambda$ -DNA translocations through a 4.3 nm ECR fabricated MoS<sub>2</sub> nanopore recorded in-situ right after pore formation at 300 mV. (b) Concatenated  $\lambda$ -DNA translocation events.



**SI Fig.10.** (a) Simplistic analytical model that relates normalized conductance drops to the ratio of the sizes of the 2 pores. Initial nanopore diameters are set to  $d_1=4.2$  nm and  $d_2= 0.1$  nm. We varied the sizes of the both pores while keeping the total conductance fixed. (b) Percentage of the blocked ionic current as a function of nanopore diameter. More rigorous model is provided by Garaj et al. <sup>6</sup>. Surprisingly our simplistic model agrees well with Garaj et al. <sup>6</sup>

## References

- 1 Liu, K., Feng, J., Kis, A. & Radenovic, A. Atomically thin molybdenum disulfide nanopores with high sensitivity for DNA translocation. *ACS Nano* **8**, 2504-2511, doi:10.1021/nn406102h (2014).
- 2 Brivio, J., Alexander, D. T. & Kis, A. Ripples and layers in ultrathin MoS<sub>2</sub> membranes. *Nano Lett* **11**, 5148-5153, doi:10.1021/nl2022288 (2011).
- 3 Dumcenco, D. *et al.* Large-area Epitaxial Monolayer MoS<sub>2</sub>. *arXiv preprint arXiv:1405.0129* (2014).
- 4 Raillon, C. *et al.* Nanopore Detection of Single Molecule RNAP-DNA Transcription Complex. *Nano Lett* **12**, 1157-1164, doi:Doi 10.1021/Nl3002827 (2012).
- 5 Chung, S. H. & Kennedy, R. A. Forward-backward non-linear filtering technique for extracting small biological signals from noise. *J Neurosci Methods* **40**, 71-86 (1991).
- 6 Garaj, S., Liu, S., Golovchenko, J. A. & Branton, D. Molecule-hugging graphene nanopores. *Proc Natl Acad Sci U S A* **110**, 12192-12196, doi:10.1073/pnas.1220012110 (2013).